Research Report

97-02

A New Induction Motor Open-Loop Speed Control Capable of Low Frequency Operation

A. Munoz-Garcia, T.A. Lipo, D.W. Novotny

Wisconsin Power Electronics Research Center
University of Wisconsin-Madison
Madison WI 53706-1691

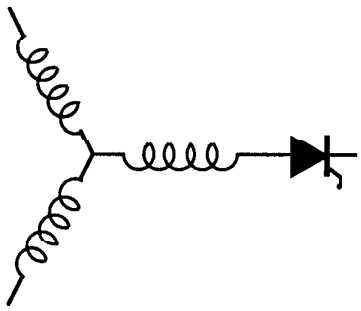

Wisconsin
Electric
Machines &
Power
Electronics
Consortium

University of Wisconsin-Madison
College of Engineering
Wisconsin Power Electronics Research Center
2559D Engineering Hall
1415 Engineering Drive
Madison WI 53706-1691

IEEE Industry Applications Society
Annual Meeting
New Orleans, Louisiana, October 5-9, 1997

A NEW INDUCTION MOTOR OPEN-LOOP SPEED CONTROL CAPABLE OF LOW FREQUENCY OPERATION

A. Muñoz-García T. A. Lipo D. W. Novotny
Department of Electrical and Computer Engineering
University of Wisconsin - Madison
1415 Engineering Drive, Madison, WI 53706-1691, USA
Tel: (608) 262-0727 Fax: (608) 262-1267 e-mail: alfredo@cae.wisc.edu http://www.cae.wisc.edu/~alfredo

Abstract* — *A novel open-loop speed control method for induction motors that provides high output torque and nearly zero steady state speed error at any frequency is presented. The control scheme is based on the popular constant volts per hertz (V/f) method using low cost open-loop current sensors. Only stator current measurements are needed to compensate for both stator resistance drop and slip frequency. The scheme proposed fully compensates for the Ir voltage drop by vectorially modifying the stator voltage and keeping the magnitude of the stator flux constant regardless of changes in frequency or load. A novel slip frequency compensation, based on a non-linear torque-speed estimate, is also introduced. This method reduces the steady state speed error to almost zero. It is also shown that a linear torque-speed approximation is a special case of the non-linear estimate and that it leads to large speed errors for loads greater than rated. It is shown that, by using the proposed method, the speed can be accurately controlled down to, at least, 1.2 Hz with load torques of more than 150% of rated value. Since the only machine parameter required, the stator resistance, is automatically measured at start up time, using the same PWM-VSI without additional hardware, the proposed drive also exhibits self-commissioning capability.

I. Introduction

The operation of induction motors in the so-called constant volts/hertz (V/f) mode has been known for many decades and its principle is well understood [1,7]. With the introduction of solid state inverters the constant V/f control became popular [2]-[4] and the great majority of variable speed drives in operation today are of this type [5]. However, since the introduction of vector control theory by Blaschke [6], almost all research has been concentrated in this area and little has been published about constant V/f operation. Its practical application at low frequency is still challenging due to the influence of the stator resistance and the necessary rotor slip to produce torque. In addition, the non-linear behavior of modern PWM-VSI in the low voltage range [8-10], makes it difficult to use constant V/f drives at frequencies below 3 Hz [11].

The simplest stator resistance compensation method consists of boosting the stator voltage by the magnitude of the Ir drop [12]. Improved techniques using the in-phase component of the stator current and a compensation proportional to a slip signal have also been proposed [7]. A vector compensation was proposed in [13], but it required both voltage and current sensors and accurate knowledge of machine inductances. More recently a scalar control scheme was proposed [14]. In this scheme the flux magnitude is derived from the current estimation. In [15] using the dc-link voltage and current both flux and torque loops are introduced. Its use at low frequency is limited by the flux estimation. Also, the slip compensation was based on a linear torque-speed assumption which led to large steady state errors in speed for high load torques. A linearized frequency compensation control based on an 'ideal induction motor' was proposed in [16].

In this paper a new stator resistance and frequency compensation technique requiring minimum knowledge of the motor's parameters is presented. The only measured quantity is the stator current. The stator resistance voltage drop is fully compensated by vectorially adding it to the commanded voltage using both in-phase and quadrature components of the stator current. The frequency compensation is based on an estimation of the air gap power and a non-linear relationship between slip frequency and air-gap power. This method predicts the correct slip frequency for any load at any frequency. The proposed control scheme requires only name-plate data, the stator resistance value, and a reasonable estimation of the break down torque. The proposed method is validated by simulation and experimental results. It is shown that large torques are obtainable even in the low speed range with almost no steady state error in speed.

II. Stator Resistance Compensation

The stator resistance compensation is based on keeping the stator flux-linkage magnitude constant and equal to its rated value. From the phasor diagram shown in Fig. 1 it is easy to show that the magnitude of E_m is

$$E_m^2 = (V_s)^2 + (I_s r_s)^2 - 2V_s(I_s r_s)\cos\phi \qquad (1)$$

Defining V_{so} as the magnitude of E_m at rated frequency f_R, at any frequency f_e^*, the required value of E_m to accomplish true constant volts/hertz is given by $V_{so}(f_e^*/f_R)$.

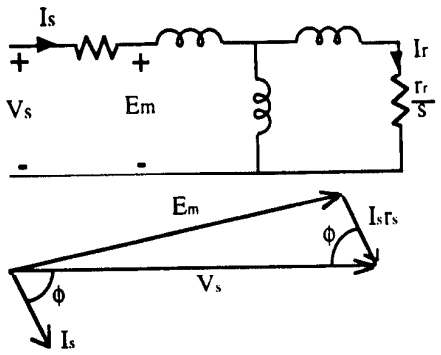

Fig. 1: Induction motor steady state equivalent circuit and phasor diagram.

Substituting this quantity into (1) yields

$$V_s = I_s r_s \cos\phi + \sqrt{\left(\frac{V_{so} f_e^*}{f_R}\right)^2 - (I_s r_s)^2 (\sin\phi)^2} \qquad (2)$$

where V_{so} is a constant defined by rated conditions and the subscript R indicates rated values.

To implement (2) the rms value of the stator current I_s, $\cos(\phi)$, and $\sin(\phi)$ are needed. Assuming a set of balanced sinusoidal currents the rms value, in terms of instantaneous quantities, can be written as

$$I_s = \sqrt{\frac{2}{3}} \sqrt{i_{as}(i_{as} + i_{cs}) + i_{cs}^2} \qquad (3)$$

The terms $\cos(\phi)$ and $\sin(\phi)$ are obtained by using a transformation similar to what is known as the complex vector form of real variables [17]. Defining the complex quantity

$$\underline{i}_s = i_{as} + \underline{a}^2 i_{bs} + \underline{a} i_{cs} \qquad (4)$$

where $\underline{a}$ is the complex number $e^{j(2\pi/3)}$. Substituting the currents and using a synchronous reference frame yields

$$\underline{i}_s^e = \frac{3\hat{I}}{2} e^{j\phi} = \frac{3}{\sqrt{2}} I_s (\cos(\phi) + j\sin(\phi)) \qquad (5)$$

where $\hat{I}$ is the peak current and ϕ the phase angle. Because of the trigonometric relation between sine and cosine and the structure of (2) only the real part of (5) is required, therefore the actual implementation does not use complex variables and (5) can be simplified to

$$Re\{\underline{i}_s^e\} = I_{s(Re)} = \sqrt{3}\left\{i_{as}\cos(\omega t - \frac{\pi}{6}) - i_{cs}\sin(\omega t)\right\} \qquad (6)$$

where $Re\{\underline{i}_s^e\}$ has been replaced by the symbol $I_{s(Re)}$ to stress that only real quantities are used.

Although by definition the rms current and the power factor are steady state quantities the use of (3), (5), and (6) yields instantaneous measurements of both of them. This is a very important factor since it gives continuous measurements that can be used for feedback purposes allowing for better dynamics in the control. An alternate form to obtain the power factor is to measure the time delay between the zero-crossings of the current and the voltage. This method however, gives poor results for several reasons; first the measured current contains high frequency noise that makes it difficult to identify the exact point of zero crossing, second the power factor measurement can only be up-dated, at most, every one sixth of a cycle. These problems are eliminated by using (3), (5), and (6). The final expression for the required stator voltage, including only instantaneously measured and commanded quantities, is

$$V_s = \frac{\sqrt{2}}{3} I_{s(Re)} \cdot r_s + \sqrt{\left(\frac{V_{so} f_e^*}{f_R}\right)^2 + \frac{2}{9}(I_{s(Re)} \cdot r_s)^2 - (I_s r_s)^2} \qquad (7)$$

Equation (7) corresponds to a vector compensation of the Ir drop. Given the inherently positive feedback characteristic of the Ir boost algorithm it is necessary to stabilize the system by introducing a first order lag in the feedback loop (low-pass filter). Since (7) contains both the Ir boost and the base V/f ratio we only need to apply the lag to the boost component of the algorithm, this is shown schematically in Fig. 2.

III. Slip Frequency Compensation

In order to produce torque an induction motor needs to develop slip. This means that the rotor only runs at synchronous speed at no load and for any other condition the mechanical speed is reduced by the slip. At rated frequency the slip is usually around 3% and its effect can be ignored. For variable frequency operation however the slip varies inversely proportional to the frequency and as the frequency decreases the slip becomes larger and it can no longer be ignored. At sufficiently low frequencies this effect becomes so important that if not adequately compensated the motor will not be able to supply the load torque and will stall.

The compensation technique used here is explained with the help of Fig. 3. Given the torque-speed curve defined by the solid line and assuming a load torque T_L the motor will develop a slip proportional to the length AB. If the stator frequency is boosted in such a way that a new torque-speed curve, as defined by the dashed line, is obtained then for the same load torque the motor will run at ω_0 which

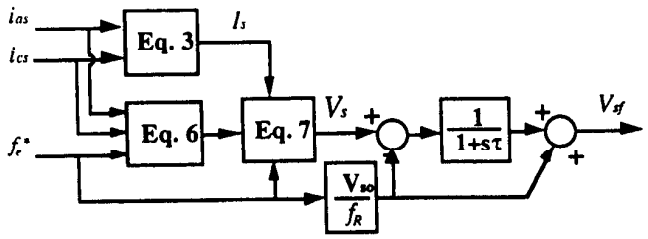

Fig. 2: Ir compensation including first order lag.

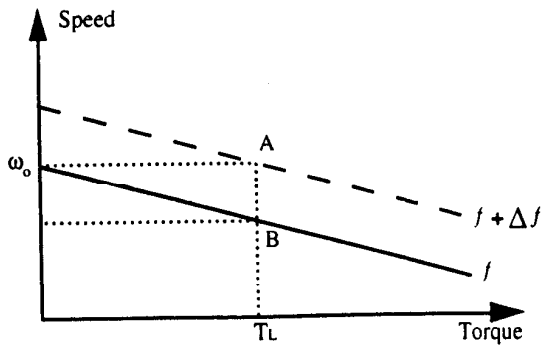

Fig. 3: Slip compensation method.

corresponds to the original synchronous speed. By adjusting the stator frequency continuously the mechanical speed can be maintained constant for any load.

In order to implement this scheme it is necessary to know the relationship between torque and slip (this is the length AB). This is normally done by assuming a linear relationship between torque and slip. Although this technique gives good results for high speeds its usefulness at low frequency and large torques is limited due to the large errors introduced by the linear approximation. The slip compensation proposed in this paper is based on the actual non-linear torque-speed characteristic of the machine.

One expression for the electromagnetic torque is known to be [1]

$$T_L = \frac{2T_{bd}}{\frac{s}{s_{bd}} + \frac{s_{bd}}{s}} \tag{9}$$

where T_{bd} is the break down torque and s_{bd} the slip at which it occurs. Since (9) is valid for any torque it is also valid for rated conditions. Defining $T_{bd} = K_o T_R$ and using (9) yields

$$\frac{s_{bd}}{s_R} = K = K_o + \sqrt{K_o^2 - 1} \tag{10}$$

which is the break-down slip in per unit of the rated slip. Substituting (10) into (9) and solving for the slip yields

$$s = \frac{KK_o T_R s_R}{T_L}\left[1 - \sqrt{1 - \left(T_L / K_o T_R\right)^2}\right] \tag{11}$$

Eq. (11) is the slip required to produce the electromagnetic torque T_L. To completely solve for the slip frequency we need to eliminate the load torque from (11). This is accomplished by using an alternate form of the electromagnetic torque [17]

$$T_L = \left(\frac{p}{4\pi}\right)\frac{P_{gap}}{f_m^* + f_{slip}} \tag{12}$$

where p is the number of poles, P_{gap} is the power transferred across the air-gap, f_{slip} is the slip frequency, and f_m^* is the mechanical commanded frequency. Substituting (12) into (11) and solving for the slip frequency yields

$$f_{slip} = \frac{1}{2 - A \cdot P_{gap}}\left(\sqrt{\left(f_m^*\right)^2 + \frac{K \cdot s_{lin}}{2K_o} P_{gap} - B \cdot P_{gap}^2} - f_m^*\right) \tag{13-a}$$

$$f_{slip} = \frac{B}{A \cdot f_m^*} \qquad \text{if } A \cdot P_{gap} = 2 \tag{13-b}$$

where the constants A and B are defined as

$$A = \left(\frac{p}{4\pi K K_o T_R s_R f_R}\right) \qquad B = \left(\frac{p}{4\pi K_o T_R}\right)^2$$

In contrast, the widely used linear torque-speed approximation [15]-[16] yields a simpler expression given by

$$f_{slip} \approx \frac{1}{2}\left(\sqrt{\left(f_m^*\right)^2 + s_{lin} P_{gap}} - f_m^*\right) \tag{14}$$

where

$$s_{lin} = \left(\frac{p}{\pi}\right)\frac{s_R f_R}{T_R} = \text{constant}$$

Notice that when K_o is large A and B become small and (13) converges to (14). The physical meaning of this is that the linear approximation assumes a machine with an infinite break-down torque. Although the exact value of K_o is not generally known it certainly is a finite quantity and, for a typical NEMA B design its value lies between 1.5 and 3. Hence the use of (13) provides a huge improvement over the linear approximation. To illustrate the difference between (13) and (14), actual and estimated torque-speed curves using both schemes are presented in Fig. 4. A 20% error on K_o has been intentionally added to the non-linear prediction. If the correct value of K_o were to be used there would be no error and the non-linear prediction would lie on top of the actual curve.

As shown in Fig. 4 the error introduced by the linear approximation is reasonably small for torques less than rated value but the error increases very rapidly for larger torques. On the other hand the non-linear approach gives much smaller errors even using an incorrect estimate of the break down torque. The difference becomes even more important at torques larger than rated value.

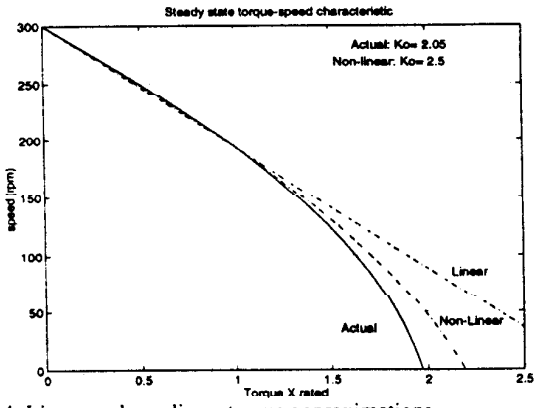

Fig. 4: Linear and non-linear torque approximations.

IV. Air-Gap Power Measurement

Given the importance of the air-gap power in the implementation of the frequency compensation algorithm, the measurement procedure will be discussed here in some detail. This power is defined by

$$P_{gap} = 3V_s I_s PF - 3I_s^2 r_s - P_{core} \tag{15}$$

where PF is the power factor and P_{core} the total core losses.

If the commanded and terminal voltages are equal the first term of (15) is obtained using (3) and (6). The second term is readily available from the current measurement (3). The last term needs some additional consideration. In general the core loss under variable frequency operation is difficult to obtain but it can be approximated from the knowledge of rated values and constant flux density operation. The core loss at rated conditions is

$$P_{core_R} = P_{in_R}(1-\eta_R) - 3I_{s_R}^2 r_s - 3I_{r_R}^2 r_r \tag{16}$$

where η_R is the rated efficiency (name-plate data). It is not difficult to show that for rated load

$$3I_{r_R}^2 r_r = \frac{s_R}{1-s_R} P_{out_R} \tag{17}$$

and substituting (17) into (16) yields

$$P_{core_R} = P_{in_R}\left(1 - \frac{\eta_R}{1-s_R}\right) - 3I_{s_R}^2 r_s \tag{18}$$

where s_R is the rated slip and P_{in_R} is the total input power at rated conditions. It is common practice to separate the core loss into hysteresis and eddy current components. This separation takes the form [18]:

$$P_{core_R} = K_h B_R^2 f_R + K_e B_R^2 f_R^2 \tag{19}$$

where K_h and K_e depend on the core type, B_R is the rated flux density, and f_R the rated frequency.

For constant flux operation (ideal V/f) these losses only vary with frequency. Assuming that at rated conditions both components are equal, after some manipulation, the total core loss at any frequency can be written in terms of its rated value as:

$$P_{core} = \frac{1}{2}\left(\frac{1+s}{1+s_R}\left(\frac{f_e^*}{f_R}\right) + \frac{1+s^2}{1+s_R^2}\left(\frac{f_e^*}{f_R}\right)^2\right) P_{core_R} \tag{20}$$

Substituting (20) into (15) gives the air-gap power as a function of commanded frequency and measured variables. The slip measurement required in (20) is obtained from (13).

V. Simulation and Experimental Results

The proposed control scheme was first simulated and then implemented in the lab. The simulations were carried out using MATLAB and ACSL.

To validate the proposed control method the algorithms were implemented using a commercial inverter and a standard 3 Hp NEMA-B machine whose parameters are listed in the Appendix. The control software was developed on a Motorola 56000 DSP system which replaced the microprocessor in the inverter. The only machine data required by the software are the rated voltage and current, number of poles, Hp rating, and nominal frequency.

The real time control and measurement program was written in Assembly language. The sampling time was chosen as 135 μs and the total control program execution time is approximately 100 μs. A complete block diagram of the proposed V/f algorithm is shown in Fig. 5 while the experimental set-up is shown in Fig. 6.

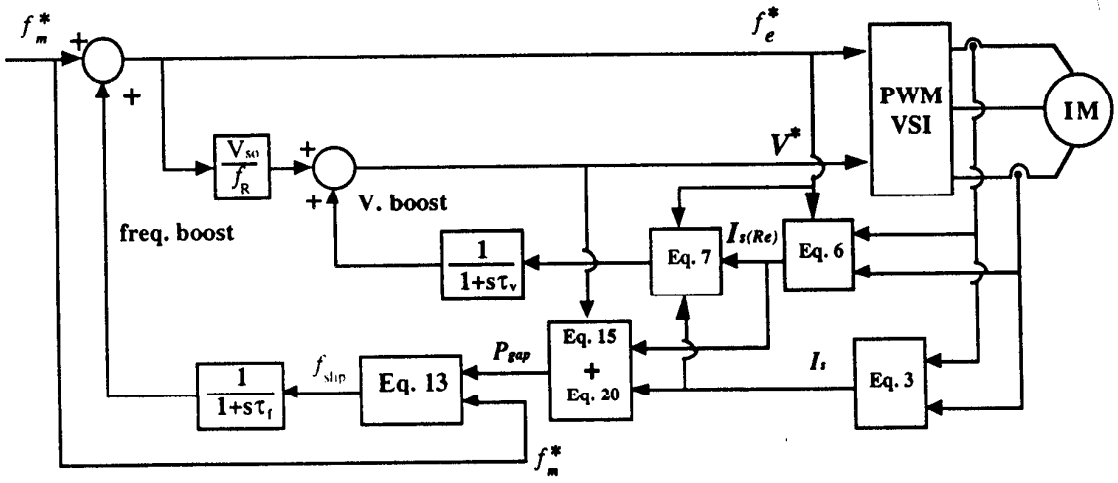

Fig. 5: Advanced induction motor V/f control, including voltage boost and slip frequency compensation loops.

A. Ir Compensation

The effectiveness of the stator resistance compensation algorithm was evaluated by looking at the resultant torque-speed characteristics at different frequencies and verifying that the slope of the curves remains constant.

The simulated results are shown in Fig. 7 and the experimental measurements are presented in Fig. 8. An excellent response in both cases is clearly seen. The lower limit on the frequency used in the experimental part is due to the machine stalling at lower frequencies.

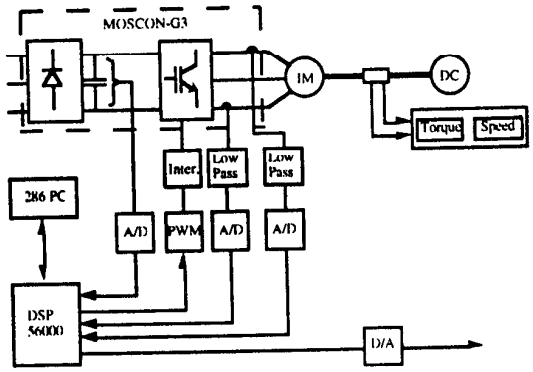

Fig. 6: Experimental set-up.

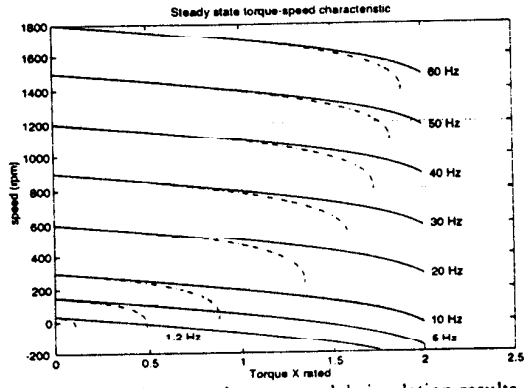

Fig. 7: Ir compensation, steady state model simulation results. Solid line: Including Ir compensation algorithm. Dotted line: without Ir compensation.

B. Slip Compensation

Both the linear and non-linear slip compensation techniques were simulated and tested in the lab. The speed range used in the experimental part was from 1.2 Hz (36 rpm) to 60 Hz (1800 rpm) for loads up to 150% of rated value. The lower limit on the frequency was primarily imposed by the capability to accurately synthesize the commanded voltage with the PWM inverter.

1) Steady State Response: The simulation results are shown in Fig. 9. As predicted the linear slip compensation yields large speed errors for torques beyond rated value. For the non-linear method a 20% error on the estimated break-down torque has been intentionally introduced. It can be seen

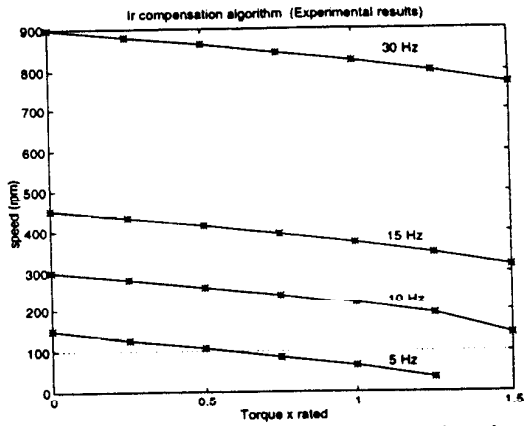

Fig. 8: Speed response including the Ir compensation algorithm. Experimental results.

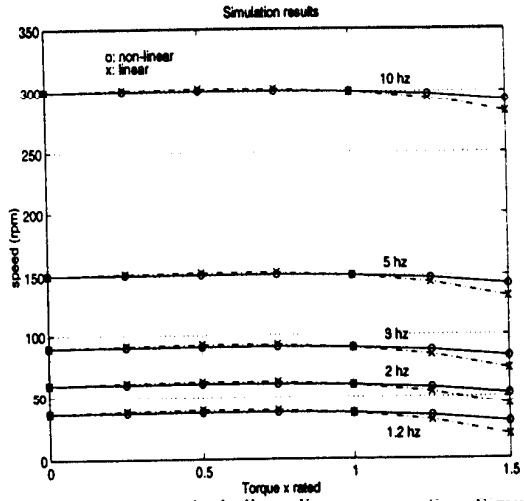

Fig. 9: Speed response including slip compensation Simulation results. Solid line: non-linear method. Dotted line: linear approximation.

that the technique is very insensitive to errors in this parameter. Fig. 10 shows the measured torque-speed curves using the non-linear slip compensation. The measured magnitude of the stator currents for the same conditions are presented in Fig. 11.

To illustrate the importance of the slip compensation method measurements at 10Hz are presented in Table I. As shown the non-linear method gives nearly zero speed error while the linear approximation yields almost a 6% error.

TABLE I
MEASURED SPEED RESPONSE AT 10 Hz

Torque (%)	No compensation speed (rpm)	Linear compensation speed (rpm)	Non-linear compensation speed (rpm)
100	235	290	298
150	173	283	299

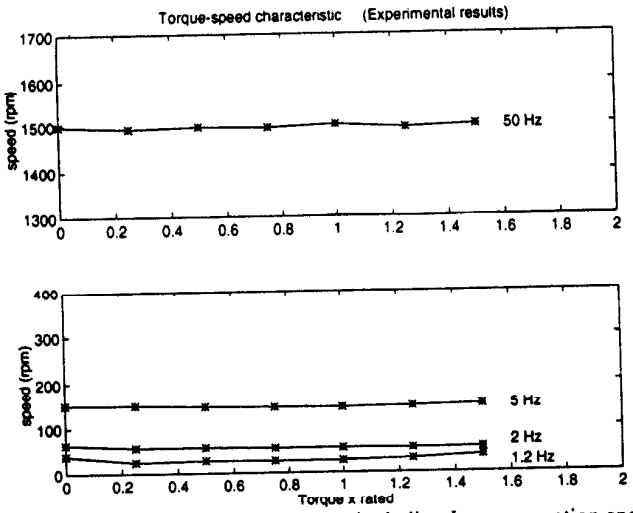

Fig. 10: Steady state speed response including Ir compensation and slip compensation. Experimental results.

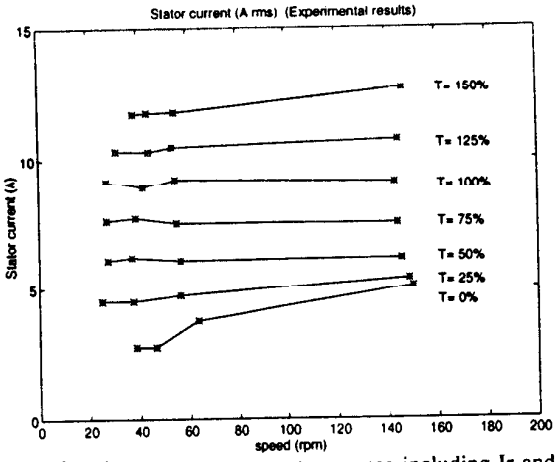

Fig. 11: Steady state stator current response including Ir and slip compensation. Experimental results.

2) Dynamic Behavior: Although constant V/Hz drives are not intended for high performance drives and its dynamic response is not of primary concern the drive must exhibit a reasonable dynamic response and avoid instability problems.

Simulation results showing the response to a rated torque change at 1.2 Hz and to a ramp speed command are presented in Figs. 12 and 13. In the first case the motor initially stalls after the load is applied and after 1 second the drive recovers and reaches the final speed with zero steady state error. The response to a ramp command shows a good dynamic behavior.

Fig. 14 shows the experimental response to a rated torque at 7 Hz commanded frequency and Fig. 15 shows the response at 2 Hz. In both cases the dynamic response is reasonable fast and very stable. Finally Fig. 16 shows the acceleration from 0 to 30 Hz.

The experimental results show the excellent response achieved with the proposed control method even at extremely low frequencies. Also the dynamic response indicates very good behavior over the whole frequency range.

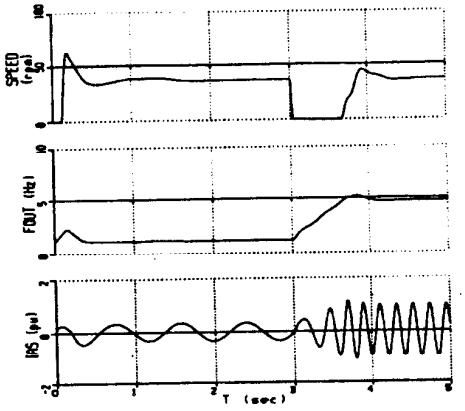

Fig. 12: Simulated no-load start at 1.2 Hz commanded frequency. Full load applied at t= 3 sec. A 10% break-away torque at zero speed is included. Top trace: Rotor speed in rpm; Middle trace: Stator frequency in Hz; Bottom trace: Instantaneous phase a stator current in per unit of rated current.

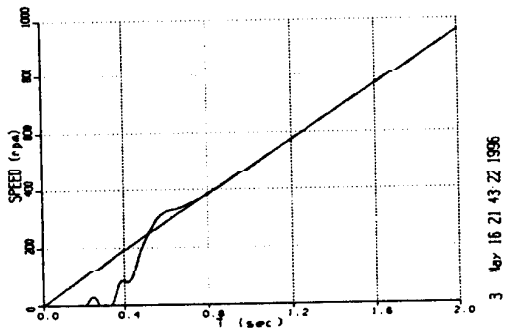

Fig. 13: Simulated response to a ramp command with full load.

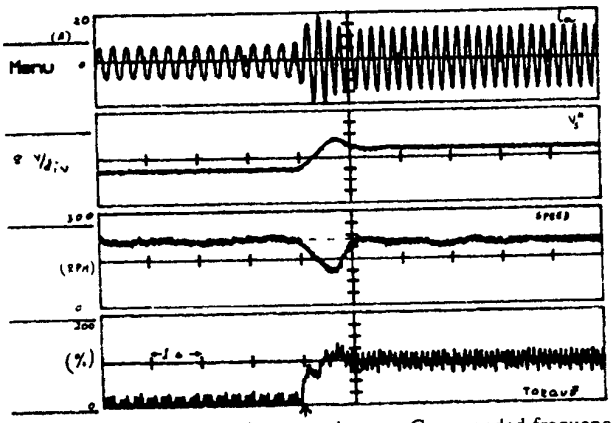

Fig. 14: Experimental rated torque change. Commanded frequency 7 Hz. Speed error 0.27%. From top to bottom: Stator current, commanded voltage (magnitude), speed, torque.

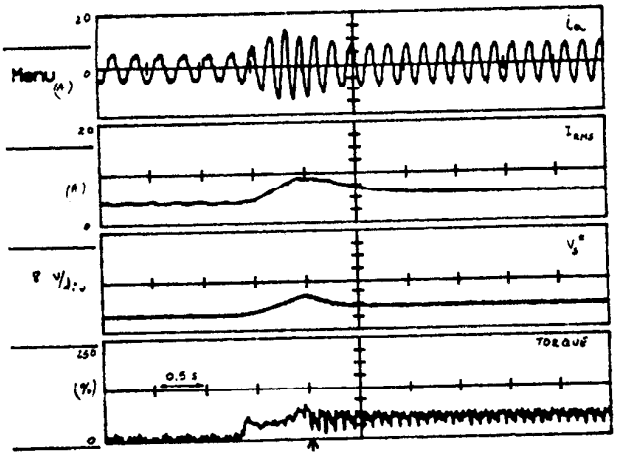

Fig. 15: Experimental rated torque change. Commanded frequency 2 Hz. Speed error 3 rpm. From top to bottom: Stator current, rms current, commanded voltage (magnitude), torque.

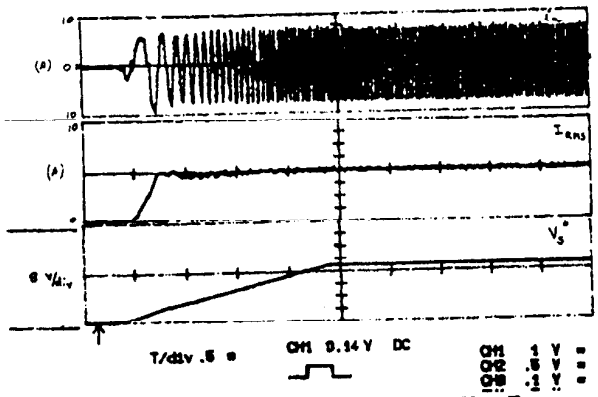

Fig. 16: Experimental acceleration from 0 to 30 Hz. From top to bottom: Stator current, rms current, commanded voltage (magnitude).

VI. Stator Resistance Measurement

As it was pointed out in the introduction the only machine parameter required to implement the control algorithm is the stator resistance. This parameter is measured during start-up using the same PWM-VSI inverter.

The stator resistance is measured by applying a dc voltage between two of the stator phases and leaving the third one disconnected. The dc voltage is synthesized using the same PWM inverter and commanding a constant voltage. By commanding $+V_{test}$ to one phase and $-V_{test}$ to another the line-line voltage contains a dc component ($2*V_{test}$) plus high frequency components starting at twice the switching frequency.

The measurement procedure is as follows: after applying the test voltage the measurement algorithm waits for approximately 0.6 seconds before starting the current measurement routine, this is done to avoid the influence of transients during the measurement . After the waiting period the current is sampled 4096 times over a time interval of approximately 0.5 seconds and the average value is computed. The stator resistance is obtained by dividing the applied voltage by the current.

This procedure yields very good accuracy with errors less than 2%. The accuracy of the method is basically defined by the accuracy of the current sensor and the quality of the synthesized output voltage. In this case the accuracy of the current sensors is fixed at 1%. The accuracy of the output voltage is guaranteed by using a dc-link voltage measurement and adjusting the value of V_{test} accordingly. The repeatability of the test is excellent yielding results that are consistent to a fraction of a percent.

The actual voltage and current wave forms obtained in the experimental set up are shown in Fig. 17. From top to bottom the traces in this Fig. are: phase current, commanded voltage, and measuring flag. The measurement is carried out when the flag is high. From this Fig., the need to wait for the transient response to die out before carrying out the measurement is clear.

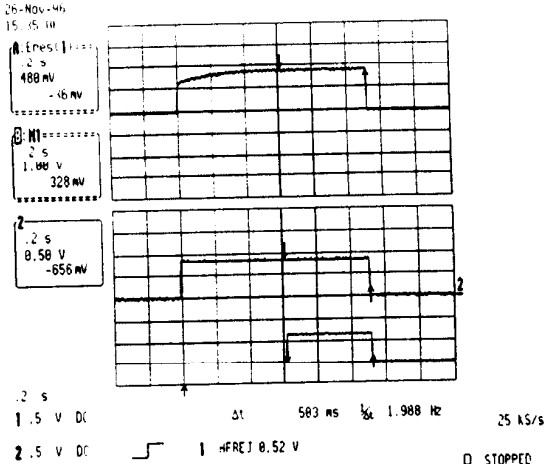

Fig. 17: Stator resistance measurement. From top to bottom: phase-a current, phase-a commanded voltage, and measurement flag (high means current acquisition).

VII. Inverter Non-Linearity

Since an accurate voltage control is essential to accomplish low frequency operation and, as mentioned earlier, an accurate synthesis of a reduced output voltage is limited by the non-linear behavior of a PWM-VSI [8-10], it is necessary to provide some means of compensation. The main effects that need to be compensated are the dead-time and the voltage drop across the switches. A detailed discussion of the compensation scheme used goes beyond the scope of this paper and it will be presented in a future publication. However, it is important to mention that in order to achieve a precise speed control in the low frequency region a voltage

accuracy better than 1 V is required. It is also important to point out that since the actual blanking time varies with device's temperature and current, the resulting variation in turn-on and turn-off delays requires that the dead-time compensation must be implemented on-line.

VIII. Conclusions

A new open loop constant V/Hz control method has been presented. The influence of the slip regulation, too often neglected, has been studied in detail and a new compensation method requiring knowledge of only the stator resistance has been proposed. The only measurement needed is the stator current which is accomplished using a low cost open-loop type of current transducer. Experimental and simulation results validate the effectiveness of the method and show that good open loop speed regulation can be achieved. The proposed drive can be easily implemented in existing V/f drives by modifying only the software. Since the only machine parameter needed for the control algorithm is the stator resistance, which is measured during start-up using the same PWM inverter and control microprocessor, the system is well suited for operation with off-the-shelf motors without needing a re-tuning of the control loops if the motor is replaced. Thus the proposed drive also exhibits self-commissioning capability.

Appendix

Parameters of the Machine Used in the Study

TABLE II
INDUCTION MACHINE DATA

3 Hp	$r_s = 0.89\ \Omega$ (1)
230 V	$r_r = 0.73\ \Omega$ (2)
9 A	$L_s = 0.065$ H (2)
60 Hz	$L_r = 0.065$ H (2)
1740 rpm	$L_m = 0.062$ H (3)

(1): DC measurement; (2): Locked rotor test; (3): No-load test

Acknowledgment

The authors would like to thank the Wisconsin Electric Machines & Power Electronics Consortium, WEMPEC, for its partial financial support to develop this project.

References

[1] Induction Machines, (book) P. L. Alger, Gordon and Breach Science Publishers, Second edition, 1970

[2] R. A. Hamilton and G. R. Lezan, 'Thyristor adjustable frequency power supplies for hot strip mill run-out tables', IEEE Trans. on Industry and general applications, Vol. IGA-3, No. 2, pp. 168-175, 1967

[3] W. Slabiak and L. Lawson, 'Precise control of a three-phase squirrel cage induction motor using a practical cycloconverter', IEEE Trans. on Industry and general applications, Vol. IGA-2, No. 4, pp. 274-280, 1966

[4] W. Shepherd and J. Stanway, 'An experimental closed-loop variable speed drive incorporating a thyristor driven induction motor', IEEE Trans. on Industry and general applications, Vol. IGA-3, No. 6, pp. 559-565, 1967

[5] Power Electronics and Variable Frequency Drives, (book) Edited by Bimal K. Bose, IEEE Press, 1996

[6] F. Blaschke, 'The principle of field orientation as applied to the new transvektor closed-loop control system for rotating-field machines', Siemens Review, Vol. 34, pp. 217-220, 1972

[7] A. Abbondanti, 'Method of flux control in induction motors driven by variable frequency, variable voltage supplies', IEEE/IAS Intl. Semi. Power Conv. Conf., pp. 177-184, 1977

[8] Y. Murai, T. Watanabe, and H. Iwasaki, 'Waveform distortion and correction circuit for PWM inverters with switching lag-times', IEEE Trans. on Ind. Appl., Vol. 23, No. 5, pp. 881-886, 1987

[9] J. W. Choi, S. I. Yong, and S. K. Sul, 'Inverter output voltage synthesis using novel dead time compensation', IEEE Trans. on Ind. Appl., Vol. 31, No. 5, pp. 1001-1008, 1995

[10] R. Sepe and J. Lang, 'Inverter nonlinearities and discrete-time vector current control', IEEE Trans. on Ind. Appl., Vol. 30, No. 1, pp. 62-70, 1994

[11] K. Koga, R. Ueda, and T. Sonoda, 'Achievement of high performances for general purpose inverter drive induction motor system', IEEE/IAS Conference record, pp. 415-425, 1989

[12] F. A. Stich, 'Transistor inverter motor drive having voltage boost at low speeds', U.S. Patent 3,971,972; 1976

[13] A. Abbondanti, 'Flux control system for controlled induction motors', U.S. Patent No. 3,909,687; 1975

[14] T. C. Green and B. W. Williams, 'Control of induction motor using phase current feedback derived from the DC link', Proceedings of the EPE'89, Vol. III, pp. 1391-1396

[15] Y. Xue, X. Xu, T. G. Habetler, and D. M. Divan, 'A low cost stator oriented voltage source variable speed drive', IEEE Ind. Appl. Society 1990 Annual Conf. Rec., pp. 410-415, 1990

[16] K. Koga, R. Ueda, and T. Sonoda, 'Constitution of V/f control for reducing the steady state speed error to zero in induction motor drive system', IEEE/IAS Conference record, pp. 639-646, 1990

[17] Vector Control and Dynamics of AC Drives, (book) D. W. Novotny and T. A. Lipo, Clarendon Press-Oxford, 1996.

[18] S. Nishikata and D. W. Novotny, 'Efficiency considerations for low frequency operation of induction motors', IEEE Ind. Appl. Society 1988 Annual Conf. Rec., pp. 91-96, 1988